X-ray views of neutron star low-mass X-ray binaries

Sudip Bhattacharyya

Department of Astronomy and Astrophysics, Tata Institute of Fundamental Research, Mumbai 400 005, India

A neutron star low-mass X-ray binary is a binary stellar system with a neutron star and a low-mass companion star rotating around each other. In this system the neutron star accretes mass from the companion, and as this matter falls into the deep potential well of the neutron star, the gravitational potential energy is released primarily in the X-ray wavelengths. Such a source was first discovered in X-rays in 1962, and this discovery formally gave birth to 'X-ray astronomy'. In the subsequent decades, our knowledge of these sources has increased enormously by the observations with several X-ray space missions. Here we give a brief overview of our current understanding of the X-ray observational aspects of these systems.

Keywords: Companion star, neutron star, stellar system, X-ray astronomy, X-ray binaries.

Introduction

COSMIC objects emit in diverse electromagnetic wavelengths, from radio to γ-rays. Some of them (e.g. stars) are luminous primarily in a narrow wavelength range, while others (e.g. active galactic nuclei) emit in a broad energy spectrum. It is, therefore, essential to observe a celestial source in various wavelengths in order to fully understand its nature. Up to the middle of the 20th century, visible light was the primary window for observation. But in the last few decades, wavelength-based branches of astronomy have not only been developed, but also have matured. Moreover, many new types of sources have been discovered by the observations in wavelengths other than visible light. One such discovery was made in X-rays using rocket-borne instruments in 1962 (ref. 1). These instruments detected X-rays from sources outside the solar system for the first time, and specifically discovered a new type of source, Scorpius X-1. This discovery brought a new era in astronomy, and formally gave birth to a new branch called 'X-ray astronomy'. Scorpius X-1 was the first observed X-ray binary, and more specifically, it was the first detected low-mass X-ray binary system containing a neutron star and a low-mass stellar companion.

e-mail: sudip@tifr.res.in

Unlike the optical (i.e. visible light) and radio detection instruments, the X-ray instruments must be sent above the atmosphere for observations. This is because X-rays from space cannot reach the surface of the earth. In the 1960s, balloons and sub-orbital rockets were extensively used to lift the X-ray instruments. However, as these carriers are short-lived, satellites were thought to be ideal for X-ray observations. The first astronomical satellite, *Uhuru* was launched by NASA in 1970. It identified over 300 discrete X-ray sources. NASA's *Einstein* satellite (launched in 1978) was the first fully imaging X-ray telescope put into space. Its few arcsecond angular resolution increased the sensitivity enormously, and made the imaging of extended objects, and the detection of faint sources possible. The *ROSAT* satellite launched in 1990 by the German/US/UK collaboration, made the first X-ray all-sky survey using a highly sensitive imaging telescope, and detected more than 150,000 objects. The scientific outcome of these key X-ray space missions, as well as the other past X-ray satellites, has revolutionized our knowledge of the X-ray sky.

The current primary X-ray space missions are: (1) NASA's *Rossi X-ray Timing Explorer* (*RXTE*); (2) European Space Agency's *XMM-Newton*; (3) NASA's *Chandra*, and (4) Japan's *Suzaku*. They primarily operate in the ≈1–10 keV range (i.e. soft X-rays), and contain a variety of instruments. The primary instrument of *RXTE* is a set of five proportional counters (called the Proportional Counter Array or PCA) with large collecting area and good time resolution (≈ 1 μs). Therefore, PCA is an ideal instrument to study the fast timing phenomena, as well as the continuum energy spectrum. However, it is not an imaging instrument, and due to poor energy resolution, PCA is not suitable to study spectral lines. This instrument operates in 2–60 keV band, although the effective collecting area becomes small above ≈ 20 keV. Another useful instrument of *RXTE* is the All-Sky Monitor or ASM. It consists of three relatively low-sensitivity proportional counters with a large field of view, and hence monitors the entire sky to detect transient X-ray sources. *XMM-Newton* contains X-ray telescopes, charge-coupled devices and high resolution Reflection Grating Spectrometers (RGS). Therefore, this satellite, operating in ≈ 0.2–12 keV range, is a good imager, and is ideal for spectral analysis. The *Chandra* observatory contains an X-ray telescope, charge-coupled devices, high resolution

camera and transmission gratings. Its angular resolution (~sub-arcsecond) is the best among all the past and current X-ray instruments, which makes it a unique imager. *Chandra* is also ideal to detect and study narrow spectral lines, and it operates in ≈0.1–10 keV. Finally, the *Suzaku* satellite also has X-ray telescopes and charge-coupled devices. Since it contains an additional Hard X-ray Detector (HXD), Suzaku can study the broadband energy spectrum.

All these X-ray space missions, especially the current ones, have gathered a wealth of information about the low-mass X-ray binary systems, and hence our understanding of these sources has grown enormously. Here, we give a brief overview of the X-ray observational aspects of neutron star low-mass X-ray binaries. We note that the reference list will not be exhaustive in this short review.

Neutron stars

Neutron stars are extremely compact objects with a mass of about one solar mass ($M_\odot$), but a radius of ~10 km. The core density of neutron stars is 5–10 times the nuclear density, and their magnetic field can be anywhere between 10^7–10^{15} Gauss. They can spin with a wide range of frequencies: very slow to several hundred Hertz. Study of these stars provides a unique opportunity to probe some extreme aspects of the universe, that cannot be achieved by other means.

Although the neutron stars were discovered in 1967, their plausible existence was predicted in the 1930s. Around this time, Subrahmanyan Chandrasekhar calculated the upper limit of the mass of a collapsed star (white dwarf) that is supported by the electron degeneracy pressure against gravity. This limit is the celebrated 'Chandrasekhar mass limit', with a value of about $1.4\,M_\odot$. If the mass of the collapsed star is greater than this limit, then the star is expected to collapse more. But if the mass is less than a certain value, the neutron degeneracy pressure will eventually balance the gravity to form a stable star, known as the neutron star[2,3]. This remained as a theoretical calculation almost for three decades, after which Hewish *et al.*[4] reported the discovery of a 1.377 s period radio pulsar at 81.5 MHz, and Gold[5,6] showed that the pulsars are spinning neutron stars with large surface magnetic fields.

The density of a neutron star increases by ≈14 orders of magnitude from the surface to the centre. As a result, the constituents and their properties change dramatically with the radial distance (see, for example ref. 7). The dense core of a neutron star may contain pion condensates, deconfined quarks, or other exotic (and possibly unknown) forms of matter, which makes the study of this part of the star extremely interesting. Moreover, according to a model, some of the neutron stars are actually 'strange stars' made entirely of u, d and s quarks[8]. Unfortunately, in spite of many theoretical studies, the properties of matter in the core of a neutron star are not yet known, because such a dense degenerate matter cannot be created in the laboratory. Perhaps the only way to understand the nature of this high-density matter is to constrain the theoretically proposed equation-of-state models of the stellar core. This can be done by measuring three independent structural parameters (e.g. mass, radius, spin frequency) of the same neutron star, because the stable stellar structure gives a single mass vs radius of curve for a known spin frequency and a given equation-of-state model[9]. Measurement of the stellar parameters is, therefore, a primary goal of the neutron star astronomy. Such a measurement, especially of the radius, is an extremely formidable task. This can be appreciated from the fact that we need to measure the ~10 km radius of a neutron star with <5% error, while the typical distance of the star is ~10^{17} km.

Neutron stars can emit in various wavelengths depending on their properties and the systems they are in. They are observed as radio, X-ray and γ-ray pulsars (that may create pulsar wind nebulae), millisecond pulsars in binary systems, magnetars, and so on, and can be found in supernova remnants, X-ray binaries, etc. In this review we will concentrate on neutron stars in X-ray binaries.

Low-mass X-ray binary

A low-mass X-ray binary (LMXB) is an old binary stellar system (typical age ~10^9 years) with a low-mass companion star (≤$1\,M_\odot$; main sequence star, evolved star or white dwarf) and a primary compact star (neutron star or black hole) rotating around each other. In such a system, the companion star fills its Roche lobe, i.e. the critical equipotential surface (see Figure 1), and matter from it flows towards the compact star. Because of the initial angular momentum, this matter cannot move radially towards the primary star, and follows slow spiral paths that form an accretion disk. In this review, we consider the systems with neutron stars as the primary stars. In such neutron star LMXBs, the accreted matter eventually hits the stellar surface and generates electromagnetic radiation. The accretion disk also emits such radiation by viscous dissipation, and both these emissions are powered by the gravitational potential energy release. The inner part of the accretion disk, as well as the neutron star surface, emit X-rays, as their typical temperature is ~10^7 K. Figure 2 gives an artist's impression of such a system. In the next section, we will give the basic theory of a simple, geometrically thin accretion disk in Newtonian gravity. Note that a more realistic approach may include complicated fluid dyanamical processes (e.g., Mukhopadhyay[10], Mukhopadhyay *et al.*[11]) and general relativistic effects (e.g., Mukhopadhyay and Misra[12]). Moreover, the magne-

tosphere of the neutron star can affect the accretion process depending on the accretion rate and the magnetic field strength. Ghosh *et al.*[13] and Ghosh and Lamb[14] provided an important theoretical understanding of this process. Due to accretion-induced angular momentum transfer, the neutron stars in LMXBs are expected to be spun-up. This is consistent with the observed stellar spin frequencies (typically ~300–600 Hz). The magnetic fields of these neutron stars are relatively low ($\approx 10^7$–10^9 Gauss) compared to the expected fields of these stars when they are born, and several groups have worked on this problem of stellar magnetic field evolution[15–20]. Note that the low magnetic field allows the accretion disk to approach very close to the neutron star. This, in combination with the fact that X-rays can be detected both from the star and the inner part of the disk for many LMXBs, provides an excellent opportunity to study the extreme physics of and around neutron stars. However, the modelling of any observation of the neutron star vicinity should consider the special and general relativistic effects, including light bending (e.g., Datta and Kapoor[21]).

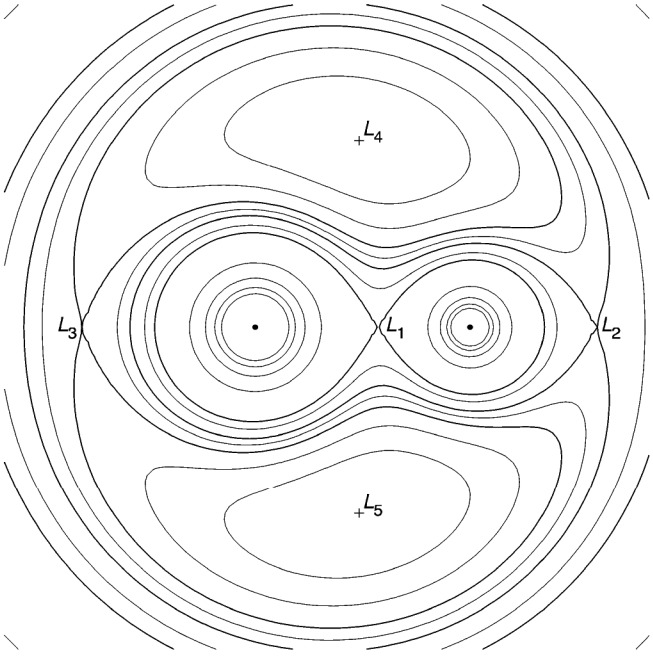

Figure 1. Sections in the orbital plane of the equipotential surfaces of a binary system with mass ratio 2 : 1. The two gravitating bodies are rotating around each other, and the above-mentioned potential includes the effects of both gravitational force and centrifugal force. The two parts of the figure-of-eight equipotential (containing the L_1 point) are called Roche lobes, and the inner Lagrange point L_1, having a saddle-like potential, allows the matter to pass from one lobe to the other (figure courtesy: Dipankar Bhattacharyya).

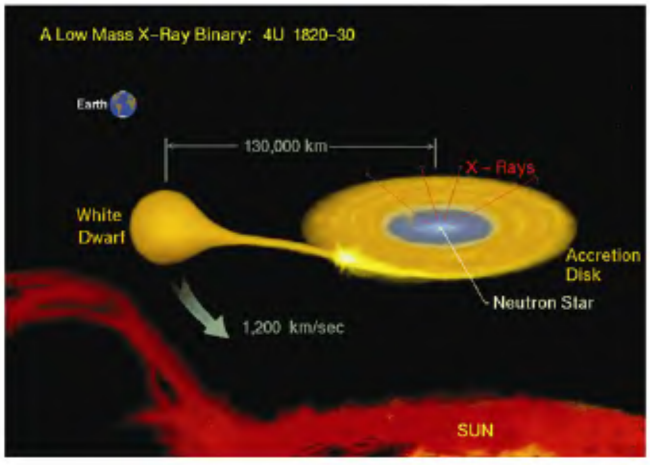

Figure 2. Artist's impression of a neutron star LMXB 4U 1820-30 (ref. 22). This is a particularly small LMXB with an orbital period of 11 min (the sun and earth are shown for an easy comparison of size). The companion is naturally a white dwarf star, because only such star can have a size similar to that of the companion's Roche lobe in these small systems (figure courtesy: Dany P. Page).

LMXBs are observed mostly in the disk, bulge and globular clusters of our galaxy. Some of them have also been discovered from the nearby galaxies, and at locations much above our galactic disk plane. According to the catalogue of Liu *et al.*[22], 187 LMXBs (containing black hole or neutron star) were known from our galaxy, 'Large Magellanic Cloud' and 'Small Magellanic Cloud' up to that time. LMXBs emit primarily in X-ray wavelengths, and the optical to X-ray luminosity ratio is normally less than 0.1 for them. The central X-ray emission from these sources cannot be spatially resolved using the current X-ray imaging instruments, because the distances of even our galactic LMXBs are very large (typically $\sim 10^{17}$ km). Therefore, in order to understand the neutron star LMXBs, we have to rely on their spectral and timing properties. In this review, we will describe some of these properties, as well as the information they provide.

Theory of accretion disk

In a neutron star LMXB, the companion mass is transferred to the neutron star typically via a geometrically thin accretion disk. Therefore, in this section we will briefly discuss the basic theory of such a disk. Here we note that the standard model of steady, thin accretion disks in Newtonian gravity was worked out by Shakura and Sunyaev[23].

In a thin accretion disk using cylindrical coordinates (r, θ, z), we expect that the θ component v_θ should be the main component of velocity, and the z component $v_z = 0$. The accreted matter should move around the neutron star with a nearly Keplerian speed (i.e. the angular speed $\Omega \approx \sqrt{GM/r^3}$; M is the mass of the neutron star), and a small radial inflow (speed $= v_r << v_\theta$) caused by the effect of viscosity should exist. We consider $\partial/\partial\theta = 0$ because of the θ-symmetry of the system. Then the equation of continuity is

$$\frac{\partial \Sigma}{\partial t} + \frac{1}{r}\frac{\partial}{\partial r}(r\Sigma v_r) = 0. \quad (1)$$

where Σ is the surface density of the accretion disk. Using this and the θ-component of the Navier–Stokes equation, we get

$$\frac{\partial}{\partial t}(\Sigma r^2\Omega)+\frac{1}{r}\frac{\partial}{\partial r}(\Sigma r^3\Omega v_r)=\Lambda, \tag{2}$$

where $\Omega = v_\theta/r$ and Λ is the term involving viscosity. We note that $2\pi r\cdot \mathrm{d}r\cdot \Sigma r^2\Omega$ is the angular momentum of an annulus between r and $\mathrm{d}r$. Hence eq. (2) multiplied with $2\pi r\cdot \mathrm{d}r$ shows how the angular momentum of the annulus changes by the viscous torque. Therefore,

$$\Lambda=\frac{1}{2\pi r}\frac{\mathrm{d}G}{\mathrm{d}r}, \tag{3}$$

where $G(r)$ is the viscous torque at the radial distance r. It is normally assumed that the term $\mathrm{d}v_\theta/\mathrm{d}r$ gives the velocity shear. However for the accretion disk,

$$\frac{\mathrm{d}v_\theta}{\mathrm{d}r}=\frac{\mathrm{d}}{\mathrm{d}r}(r\Omega)=\Omega+r\frac{\mathrm{d}\Omega}{\mathrm{d}r}, \tag{4}$$

in which Ω is associated with pure rotation, and $r\mathrm{d}\Omega/\mathrm{d}r$ gives the shear. Therefore, the viscous stress is $\mu r\mathrm{d}\Omega/\mathrm{d}r$, where μ is the coefficient of viscosity. Then the viscous torque is

$$G(r)=\int r\,\mathrm{d}\theta\int \mathrm{d}z\,\mu r^2\frac{\mathrm{d}\Omega}{\mathrm{d}r}=2\pi\nu\Sigma r^3\frac{\mathrm{d}\Omega}{\mathrm{d}r}. \tag{5}$$

Here, $\nu=\mu/\rho$ is the kinematic viscosity and ρ is the volume density. Therefore, using eqs (2), (3) and (5), we get

$$\frac{\partial}{\partial t}(\Sigma r^2\Omega)+\frac{1}{r}\frac{\partial}{\partial r}(\Sigma r^3\Omega v_r)=\frac{1}{r}\frac{\partial}{\partial r}\left(\nu\Sigma r^3\frac{\mathrm{d}\Omega}{\mathrm{d}r}\right). \tag{6}$$

Equations (1) and (6) govern the accretion disk dynamics. If the disk is nearly Keplerian, then these two equations can be combined to get

$$\frac{\partial\Sigma}{\partial t}=\frac{3}{r}\frac{\partial}{\partial r}\left[r^{1/2}\frac{\partial}{\partial r}(\nu\Sigma r^{1/2})\right]. \tag{7}$$

This equation gives the time evolution of the accretion disk.

Let us now consider a special case, viz. a steady ($\partial/\partial t = 0$) geometrically thin accretion disk. From eqs (1) and (6) we get

$$r\Sigma v_r=C_1, \tag{8}$$

$$\Sigma r^3\Omega v_r-\nu\Sigma r^3\frac{\mathrm{d}\Omega}{\mathrm{d}r}=C_2, \tag{9}$$

where C_1 and C_2 are constants. For a steady disk, the mass accretion rate is $\dot{m}=-2\pi r\Sigma v_r$. Therefore, from eq. (8),

$$C_1=-\frac{\dot{m}}{2\pi}. \tag{10}$$

In order to calculate C_2, we consider a boundary condition

$$\frac{\mathrm{d}\Omega}{\mathrm{d}r}\Big|_{r=r_{\mathrm{in}}}=0. \tag{11}$$

Let us justify this condition for the following two cases: (1) when the disk is extended up to the stellar surface, and (2) when the star is well inside the disk, and the matter falls from the disk inner edge towards the star quasiradially. For a near-Keplerian disk, the angular speed Ω increases with the decrease of r. For the first case, since the stellar angular speed is less than Keplerian (otherwise the star would break up), the disk Ω must decrease with the decrease of r close to the star. Therefore, $\mathrm{d}\Omega/\mathrm{d}r$ must be zero at some point (assumed to be $r = r_{\mathrm{in}}$) near the stellar surface. On the other hand, for the second case, the torque at the disk inner edge is expected to vanish (note: it may not be exactly true in reality) making $\mathrm{d}\Omega/\mathrm{d}r = 0$. The region (between the star and the disk) in which the flow deviates considerably from Keplerian is called the boundary layer. From eqs (8), (9) and (11), we get

$$C_2=-\frac{\dot{m}}{2\pi}r_{\mathrm{in}}^2\Omega=-\frac{\dot{m}}{2\pi}(GMr_{\mathrm{in}})^{1/2}, \tag{12}$$

where M is the stellar mass. Substituting this in eq. (9), and using eqs (8) and (10), we get

$$\nu\Sigma=\frac{\dot{m}}{3\pi}[1-(r_{\mathrm{in}}/r)^{1/2}]. \tag{13}$$

This shows that the accretion rate is greater for larger viscosity. The viscous dissipation in the accretion disk causes emission from the disk, and the source of this emitted energy is the gravitational potential energy release. This viscous dissipation rate per unit volume of the accretion disk is $\mu r^2(\mathrm{d}\Omega/\mathrm{d}r)^2$. Integrating this over the disk thickness and assuming Keplerian angular speed, we get the rate of energy emitted per unit area of the disk from eq. (13):

$$-\frac{\mathrm{d}E}{\mathrm{d}t}=\frac{3GM\dot{m}}{4\pi r^3}[1-(r_{\mathrm{in}}/r)^{1/2}]. \tag{14}$$

Therefore, the total power emitted from a disk extending from $r = r_{\mathrm{in}}$ to infinity is

$$L=\frac{GM\dot{m}}{2r_{\mathrm{in}}}. \tag{15}$$

This shows that, for a steady, geometrically thin accretion disk in Newtonian gravity, half of the gravitational potential energy is emitted by viscous dissipation in the disk, and the rest half remains stored in the accreted matter as the kinetic energy, and gets dissipated in the boundary layer.

It is expected that a geometrically thin Keplerian disk should emit like a blackbody. Therefore, the temperature $T_{\rm eff}(r)$ of the disk surface can be calculated from eq. (14):

$$T_{\rm eff}(r) = \left\{\frac{3GM\dot{m}}{8\pi r^3\sigma}[1-(r_{\rm in}/r)^{1/2}]\right\}^{1/4}, \qquad (16)$$

where σ is the Stefan–Boltzmann constant. As the blackbody temperature varies with the radial distance, the spectrum from a disk is known as multicolour blackbody. For luminous LMXBs, the X-rays from the neutron star boundary layer and the inner part of the accretion disk can substantially irradiate the disk surface. This irradiation temperature $T_{\rm irr}(r)$ (which is the blackbody temperature) is proportional to $r^{-1/2}$ (ref. 24). Therefore, the net effective disk temperature is $T_{\rm disk}(r) = [T^4_{\rm eff}(r) + T^4_{\rm irr}(r)]^{1/4}$, in which $T_{\rm eff}(r)$ dominates for the inner portion (that emits X-rays) of the disk, and $T_{\rm irr}(r)$ dominates far away from the neutron star. Note that the latter can have significant consequences for the disk instability[24].

Selected features

Outbursts

A class of neutron star LMXBs are called transients. These sources have two distinctly different intensity states: (1) the quiescent state in which the source remains for months to years, and (2) the outburst state which continues for weeks to months (sometimes for years; e.g. for the source KS 1731-260). The luminosity of the source typically increases by several orders of magnitude as it evolves from the quiescent state into an outburst. Figure 3 shows the long-term intensity profile of such a transient 1A 1744-361, exhibiting two clear outbursts. The transient nature of these LMXBs is normally attributed to an accretion disk instability, that causes high accretion rates for certain periods of time, and almost no accretion during other times (see ref. 25, for a review). These sources are often not detectable in their quiescent states, and in some cases when they are detectable, the poor statistics due to the small number of observed photons hinders a detailed study. For most of the scientific purposes, it is therefore preferable to observe these transients during their outbursts. New transients are also typically discovered during the outburst states. However, it cannot normally be predicted when a transient will come out of its quiescent state. Therefore, instruments with large field-of-view that can monitor the entire sky almost continuously are required to find the transients in their outbursts. The *RXTE* ASM is such an useful instrument, that has discovered many new transient LMXBs, as well as detected subsequent outbursts of them.

However, there are scientific reasons that motivate the observations of transient neutron star LMXBs in their quiescent states. For example, during the quiescence, the neutron star surface should be the primary X-ray emitting component, which can be modelled to constrain the stellar radius. Besides, a long outburst heats up the neutron star crust taking it out of thermal equilibrium with the rest of the star. Therefore, tracking the LMXB system going into the quiescence, and the analysis of the quiescent X-ray data can provide a unique opportunity to probe some aspects of the neutron star extreme physics (e.g. Cackett *et al.*[26]). For example, such a study allows one to compare the observed neutron star cooling rate with the theoretical cooling curve, that involves the physics of stellar constituents. Note that the satellites (e.g. *Chandra*, *XMM-Newton*) with high sensitivity imaging instruments are used to observe the sources in quiescence.

Thermonuclear X-ray bursts

Many neutron star LMXB systems show a spectacular eruption in X-rays every few hours to days. During these bursts, the observed X-ray intensity goes up sharply in ≈0.5–5 s, and decays relatively slowly in ≈10–100 s (see Figure 4)[27]. The typical energy emitted in a few seconds during such a burst is ~10^{39} ergs (note that the sun takes more than a week to release this energy). These bursts are known as type-I or thermonuclear bursts, and were first

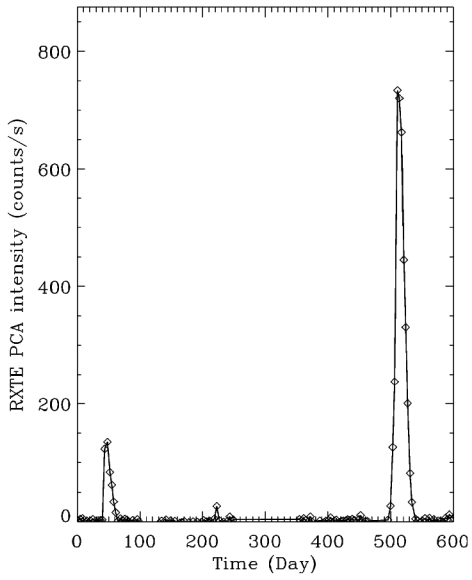

Figure 3. Long-term X-ray light curve (i.e. observed intensity profile) of a transient neutron star LMXB 1A 1744-361 showing its two outbursts[112]. The intensity is expressed in the photon count rate detected with the PCA instrument of the *RXTE* satellite.

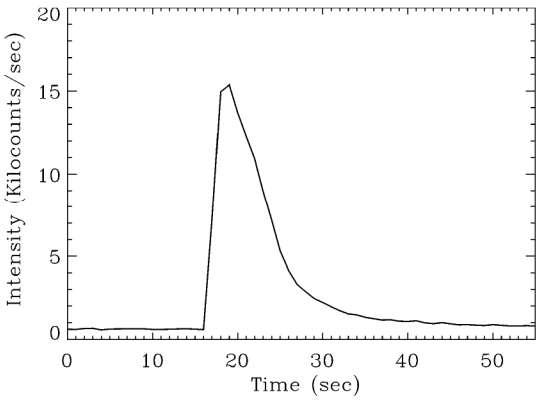

Figure 4. X-ray intensity profile of a typical thermonuclear X-ray burst observed from an LMXB. After the onset of the burst, the X-ray intensity increases quickly by more than an order of magnitude (compared to the non-burst intensity corresponding to the gravitational energy release), and then decays relatively slowly as the neutron star surface cools down.

discovered in the 1970s (refs 28 and 29). Soon after their discovery it was realized that they originate from recurrent unstable nuclear burning of accreted matter on the neutron star surfaces[27,30,31]. The neutron star surface origin was supported by the observational fact that the burst emission area (estimated from the energy spectrum of the bursts) matched with the expected surface area of a neutron star[32]. Although a competetive emission area could be the inner portion of the accretion disk, nuclear ignition in order to produce the observed bursts cannot occur in such a rare medium. But what shows that the nuclear burning causes the bursts? Before coming to that point, we would like to convince the readers that such a nuclear burning has to be unstable. This is because, while the nuclear energy released per nucleon by fusion is only a few MeV, the gravitational energy release by a nucleon falling on the neutron star surface from a large distance is GMm_{nucleon}/R (M and R are neutron star mass and radius respectively), which is typically ~200 MeV. Therefore, the energy released from a stable burning of the accreted matter would be entirely lost in the observed gravitational energy. So the nuclear burning can power the bursts, only if the accreted matter accumulates on the neutron star surface for a long time, and then burns quickly in an unstable manner. This instability appears if the nuclear energy generation rate is more temperature-sensitive than the radiative cooling rate. For an observed dataset from a given source, the ratio of the total energy content in all the bursts to that in the non-burst emission roughly tallies with the expected nuclear energy release (per nucleon) to the expected gravitational energy release (per nucleon) ratio[33]. This is one of the strongest evidences of the nuclear energy origin of the bursts. Here we note that, only a year before these bursts were discovered, Hansen and van Horn[34] predicted that thin hydrogen and helium layers on neutron star surfaces could be susceptible to the above-mentioned instability[27].

The accreted material consists of mostly hydrogen, some helium and a small amount of heavier elements, except when the donor companion is a white dwarf. This matter, that accumulates on the neutron star surface, undergoes hydrostatic compression as more and more material piles on, and the ignition density and temperature are reached in a few hours to days. The burning typically happens at a depth of ≈10 m at a column density of $\sim 10^8$ g cm^{-2}. The compression rate and the ignition depend on the accretion rate, which sets four distinct regimes of burning[33]. *Regime 1*: In most cases, the temperature of the accumulated material exceeds 10^7 K, and hence the hydrogen burns via the CNO cycle instead of the proton–proton (pp) cycle. This causes mixed hydrogen and helium bursts triggered by the unstable hydrogen ignition, which happens for the accretion rate per unit neutron star surface area $\dot{m} < 900$ g cm^{-2} s$^{-1}(Z_{\text{CNO}}/0.01)^{1/2}$ (ref. 33). Here Z_{CNO} is the mass fraction of CNO. *Regime 2*: At higher temperatures ($T > 8 \times 10^7$ K), the proton capture timescale becomes shorter than the subsequent β decay lifetimes. Hence, the hydrogen burns via the 'hot' CNO cycle of Fowler and Hoyle[35]:

$$^{12}\text{C}(p, \gamma)^{13}\text{N}(p, \gamma)^{14}\text{O}(\beta^+)^{14}\text{N}(p, \gamma)^{15}\text{O}(\beta^+)^{15}\text{N}(p, \alpha)^{12}\text{C}.$$

In this case, the hydrogen burning happens in a thermally stable manner (i.e. without triggering a thermonuclear burst) simultaneously with the accumulation of matter. This allows a helium layer to build up below the hydrogen layer. For the $\dot{m}$ range 900 g cm^{-2} s$^{-1}(Z_{\text{CNO}}/0.01)^{1/2} < \dot{m} < 2 \times 10^3$ g cm^{-2} s$^{-1}(Z_{\text{CNO}}/0.01)^{13/18}$, the hydrogen becomes entirely burned before this helium is ignited[27,33]. So when the helium ignition happens, a short (~10 s) but very intense burst occurs by the unstable triple-alpha reaction of the pure helium ($3\alpha \rightarrow {}^{12}$C). Such a burst is called a 'helium burst'. Many of these bursts are so intense that the local X-ray luminosity in the neutron star atmosphere may exceed the Eddington limit (for which the radiative pressure force balances the gravitational force), and the photospheric layers may be lifted off the neutron star surface. Such bursts are called photospheric radius expansion (PRE) bursts. *Regime 3*: For $\dot{m} > 2 \times 10^3$ g cm^{-2} s$^{-1}(Z_{\text{CNO}}/0.01)^{13/18}$, hydrogen burns via the 'hot' CNO cycle in a stable manner (as for regime 2), but enough unburnt hydrogen remains present at the time of helium ignition. This is because at this higher accretion rate, the helium ignition conditions are satisfied much sooner. Therefore in this regime, mixed hydrogen and helium bursts are triggered by helium ignition. During such a burst, the thermal instability can produce elements beyond the iron group[36–40] via the rapid-proton (rp) process of Wallace and Woosley[41]. This process burns hydrogen via successive proton capture and β decays. The long series of β decays makes these bursts typically much longer (~100 s) than the helium bursts. *Regime 4*: Finally at a very high accretion rate (comparable to the Eddington

limit), the helium burning temperature sensitivity becomes weaker than the cooling rate sensitivity[42,43]. Therefore in this regime, the stable burning sets in, and the thermonuclear bursts do not occur.

Apart from type-I X-ray bursts, another type of thermonuclear X-ray bursts with much larger recurrence time (~ years) has been observed. These are called superbursts, and they differ from the type-I bursts also in the decay time (~1–3 h) and the amount of released energy (~10^{42} ergs). The first superburst was discovered by Cornelisse *et al.*[44] from the known type-I burster 4U 1735-44. So far about 15 superbursts have been detected from 10 sources[45]. It is believed that these bursts of large fluence happen by the $^{12}C + {}^{12}C$ fusion reaction at a column depth of $\approx 10^{12}$ g cm^{-2} (refs 45–47). However, currently our understanding of superbursts is not as clear as that of type-I bursts.

Thermonuclear bursts provide a unique opportunity to study some aspects of extreme physics. Moreover, such a study brings together several branches of physics: nuclear physics, astrophysics, general theory of relativity, magneto hydrodynamics, etc. These bursts can also be useful to constrain the neutron star parameters, and hence to understand the nature of the stellar core matter at supranuclear densities (see the spectral and timing properties of these bursts in later sections). Therefore, the thermonuclear bursts belong to a truly multidisciplinary field, which is not yet well understood. One such poorly explored aspect of these bursts is the thermonuclear flame spreading on the neutron star surfaces. Burst is ignited at a certain location on the stellar surface, and then the burning region expands to cover the entire surface[48,49]. The theoretical modelling of thermonuclear flame spreading including all the main physical effects is extremely difficult, and only recently Spitkovsky *et al.*[49] have provided some insights in this field. Although these authors have ignored several physical effects (magnetic field, strong gravity, etc.) in their model, they have considered the effects of the Coriolis force, which is important as the bursting neutron stars are rapidly spinning (spin frequency ~300–600 Hz). The observational study of flame spreading is also no less difficult than the theoretical study. This is because the spreading mostly happens within ≈1 s during the burst rise, and in order to study it observationally, one needs to detect and measure the evolution of the burst spectral and timing properties during this short time. Only recently, this has been possible for a few bursts by analysing the *RXTE* PCA data[50–52]. Moreover, an indication of the effects of the Coriolis force on the flame spreading (as predicted by Spitkovsky *et al.*[49]) has also been found[53].

Type-II bursts

A series of bursts, known as type-II X-ray bursts, are observed from neutron star LMXBs in quick succession. To the best of our knowledge, only two such systems (rapid burster and GRO J1744-28) exhibit these bursts[54–56]. The intervals between the bursts vary between seconds to ~1 h, and the burst duration is in the range of seconds to minutes. The typical emitted energy range during a burst from the rapid burster is $\sim 1 \times 10^{38}$ to $\sim 7 \times 10^{40}$ ergs (ref. 57). These bursts often show successive peaks and flat tops. Note that a source is not always active for type-II X-ray bursts, and a series of such bursts are observed in certain periods of time. Type-II X-ray bursts are distinctly different from the type-I bursts in many ways. For example, the latter bursts show a spectral softening during burst decay, while the former bursts lack this signature. Type-II bursts are believed to be caused by spasmodic accretion, possibly due to an accretion instability[57]. Therefore, these bursts are powered by the gravitational energy, while the type-I bursts are powered by the nuclear energy. The recent models of the type-II bursts include the effects of magnetosphere[58] and intermittent advection-dominated accretion flow[59]. However, the origin of the accretion instability is not yet well understood.

Dips and eclipses

Some neutron star LMXBs show periodic temporary decrease in X-ray intensity. This timing feature can be divided into two distinct categories: eclipses and dips. Both of them occur with the binary orbital period, and hence provide an excellent way to measure this period[60]. Partial and total eclipses are believed to be caused by the obscuration of the X-ray source by the companion star[61]. Such an obscuration requires an observer's line-of-sight to be close to the plane of the binary system (i.e. close to the accretion disk plane). Therefore, the observation of eclipses from a source implies that its inclination angle is large (>75°)[62]. This inclination angle i is measured from the direction perpendicular to the accretion disk plane. The dips are periodic but irregular, and typically are more pronounced at lower energies[61]. The shape, depth and duration of each dipping interval vary widely from cycle to cycle, and within such an interval the observed intensity varies dramatically on a timescale of a few seconds (see Figure 5). These dips are believed to be caused by a bulge on the edge of the accretion disk at the region where the gas stream from the companion star hits the disk (see Figure 2 for a view of this impact region)[63]. Therefore, dips imply $i > 60°$ (ref. 62). The detailed nature of this bulge is still a matter of debate, and spectral analysis can shed light on this.

Spectral aspects

Continuum spectrum

Persistent emission: The study of the continuum spectrum of the persistent emission (i.e. non-burst, non-

dipping, non-eclipsing) from the neutron star low-mass X-ray binary systems can be useful to understand the various components of the accretion flow and their structures, including the flow in the strong gravity region near the neutron star. Such a spectrum can be typically fitted with two spectral components. Mitsuda *et al.*[64] used a single-temperature blackbody plus a multicolour blackbody model. The former component is expected to be produced from a boundary layer between the accretion disk and the neutron star, while the latter may be produced from the accretion disk. In an alternative two-component model, White *et al.*[65,66] used a Comptonization component instead of a multicolour blackbody. They assumed that the Comptonization component was originally the disk component which was dominated by the Comptonization processes. In the later years, it has been found that a Comptonization component is often required to fit the observed persistent emission continuum spectrum, and an additional blackbody is needed when the source is more luminous and spectrally softer (see, for example, Bhattacharyya *et al.*[67]). Apart from these, there is evidence of an extended 'accretion disk corona' (ADC) for some sources, that can be modelled with a power law[68]. However, we note that much work needs to be done in order to build a self-consistent spectral model involving all the X-ray emitting and absorbing components, and to fit the observed spectrum with such a single model.

Thermonuclear burst emission: Spectrum of a thermonuclear X-ray burst is obtained usually by subtracting the preburst emission spectrum (assumed to be powered by the gravitational energy release) from the observed spectrum during the burst[69]. The continuum burst spectra are thermal, and in most cases they are quite well described with a blackbody model[32,70]. The temperature of this blackbody naturally increases rapidly during the burst intensity rise, and then decreases relatively slowly during the burst decay. If the entire neutron star surface emits like a blackbody of the same temperature at a given time, then the neutron star radius ($R_{\rm obs}$) can, in principle, be measured from the following formula: $R_{\rm obs} = d[F_{\rm obs}/(\sigma T_{\rm obs}^4)]^{1/2}$. Here, $F_{\rm obs}$ and $T_{\rm obs}$ are the observed flux and temperature respectively, and d is the source distance, which may be known by an independent technique. Note that the measurement of the neutron star radius can be useful to understand the nature of the dense matter of the stellar core. However, in order to do such a measurement, one needs to include the following two effects. (1) The electron (Compton) scattering in the neutron star atmosphere shifts the blackbody spectrum (originated from the burning layer) towards higher energies, and changes its shape slightly[71–75]. Such a blackbody is called a 'diluted blackbody', and its temperature ($T_{\rm col}$, i.e., the colour temperature) is related with the blackbody temperature ($T_{\rm BB}$) by the colour factor f. (2) The surface gravitational redshift shifts the temperature towards a lower value. Therefore, the observed temperature $T_{\rm obs}$ is related to $T_{\rm BB}$ by $T_{\rm BB} = T_{\rm obs}(1+z)/f$. Correspondingly, the actual neutron star radius $R_{\rm BB}$ is then related to the observed radius $R_{\rm obs}$ by $R_{\rm BB} = R_{\rm obs} f^2/(1+z)$. Therefore, in order to measure the neutron star radius from the continuum burst spectra, one needs to independently estimate or measure the colour factor f and the surface gravitational redshift factor $1+z$. The former can be estimated from the temperature, surface gravity and the atmospheric chemical composition[76], while the latter can be calculated from the neutron star radius-to-mass ratio. This ratio can be independently measured from the surface atomic spectral lines or the burst oscillations (see later).

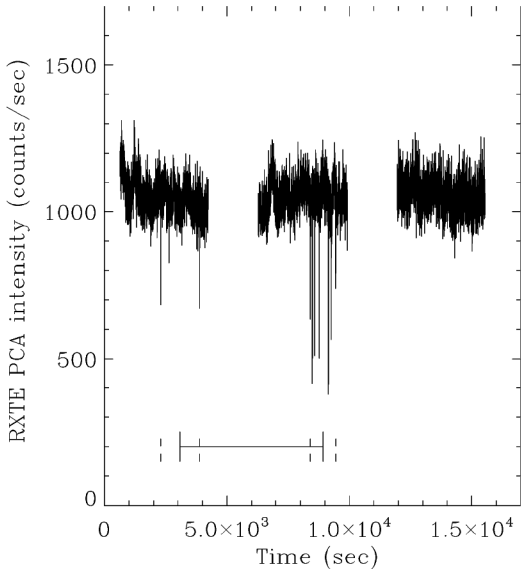

Figure 5. X-ray intensity dips observed from a neutron star LMXB 1A 1744-361 (ref. 112). The separation between two sets of consecutive dips gives the orbital period of the binary system (see text). Because of the gap in the observed data, one cannot be sure whether the two sets of dips shown in this figure are consecutive. Hence, these two sets of dips may be the orbital period or a multiple of that.

The evolution of the continuum spectrum of a thermonuclear burst can be best measured using the PCA instrument of the *RXTE* satellite. Such a measurement during the burst rise will be extremely useful to study the thermonuclear flame spreading. The chemical composition of the neutron star atmosphere may change during the burst. Therefore, and since the burst temperature also evolves, the observed radius $R_{\rm obs}$ changes substantially, and apparently irregularly during the burst decay[69]. An understanding of these changes will be essential to (1) measure the neutron star radius using the burst continuum spectrum, (2) understand the nuclear physics of bursts, and (3) probe the magnetohydrodynamics of the burning layer and the atmosphere.

Dipping emission: In order to probe the nature of the bulge that causes dips, it is essential to understand how

the continuum spectrum changes as the source goes into the dipping interval. A simple increase in the neutral absorber column density from its persistent emission value cannot explain the dip spectra. Currently, there are two competing spectral models to explain the dips. (1) The 'progressive covering' model (e.g. Church *et al.*[68]): in this approach, the X-ray emission is considered to originate from a point-like blackbody and a power-law from an extended component (e.g. a corona). The dipping is assumed to be caused by the partial and progressive covering of the extended component by a neutral absorber. (2) The ionized absorber model (e.g. Boirin *et al.*[77]): in this approach, the dips are caused by the increase in column density and the decrease in ionization state of an ionized absorber, along with a neutral absorber column density increase. This model can naturally explain some of the observed narrow spectral features.

Line spectrum

Lines from high inclination sources: Many of the high inclination neutron star LMXBs (for example, dipping sources) exhibit narrow spectral absorption features[78–80], as well as narrow recombination emission lines[81]. The most prominent of these lines are the Fe XXV and XXVI absorption lines. These spectral features are believed to originate from the material above the accretion disk, and can be observed only when the observer's line-of-sight passes through this material. This is possible only for the high inclination sources. The narrow spectral features, therefore, can be useful to constrain the structures and properties (e.g. ionization states, relative abundances of various elements) of the photoionized plasma above the accretion disks in these systems[81]. Note that, although the spectral features are mostly seen from high inclination LMXBs, this plasma must be common to all LMXBs, and hence these features will be useful in understanding LMXBs in general.

Line from disk: Broad asymmetric spectral iron emission line has been observed from many accreting supermassive and stellarmass black hole systems[82,83]. It is believed to originate from the inner portion of the accretion disk, when the disk is irradiated by a hard X-ray source (e.g. an accretion disk corona). Such an irradiation creates a 'reflection' component of the X-ray spectrum. When the hard X-ray photon enters the colder disk, it is either scattered out of the disk, or destroyed by Auger de-excitation, or reprocessed into a fluorescent line photon that escapes the disk[84]. The observed iron $K\alpha$ line near 6.4 keV is the strongest fluorescent line from such a system. As the matter in the inner accretion disk rotates fast, and is close to the black hole, Doppler effect broadens the line, special relativistic beaming makes it asymmetric, and the gravitational redshift shifts it towards the lower energies. Therefore, these lines can be useful to study the accretion flow close to the black hole, to test the theory of general relativity, and to measure the black hole spin.

For long time it has been known that the persistent spectra of many neutron star LMXBs contain broad iron emission line[85]. It was suspected that such a line might have an origin similar to that of the broad iron line from black hole systems. However, the asymmetry of these lines was not established, and hence their origin was not well understood. Recently, Bhattacharyya and Strohmayer[86] have, for the first time, established the inner disk origin of such a line from the neutron star LMXB Serpens X-1 (see Figure 6). This was later supported for several other sources (e.g., refs 87–89). Therefore, the high precision observations of the broad iron $K\alpha$ line from neutron star LMXBs could be useful to constrain the stellar parameters (radius, angular momentum) and to probe the inner accretion disk. However, evidence of the 'reflection' component of the X-ray spectrum is still marginal[89], which the theory and the future observations should address.

Line from neutron star: Observing atomic spectral lines from the surface of a neutron star has been one of the long-standing goals of the neutron star astrophysics. This is because, such an observation and the identification of the line provide the cleanest way to measure the neutron star radius-to-mass ratio using the following formula (for the Schwartzschild spacetime appropriate for a non-spinning neutron star): $E_{\rm em}/E_{\rm obs} = 1 + z = [1 - (2GM/Rc^2)]^{-1/2}$ (refs 90 and 91). Here, $E_{\rm em}$ is the emitted energy of the line photons, $E_{\rm obs}$ is the observed energy of these

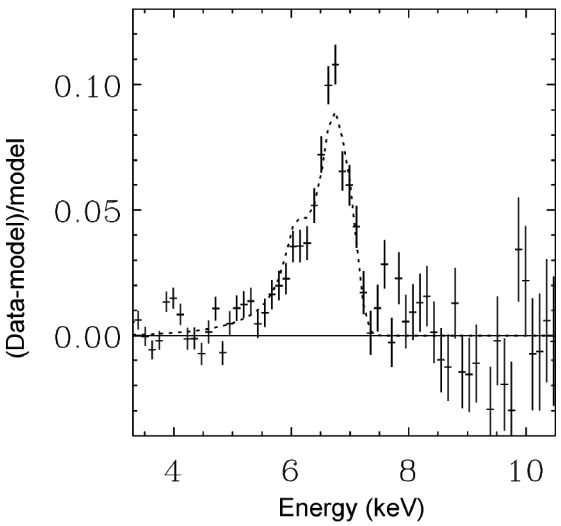

Figure 6. Broad relativistic iron (Fe Kα) spectral line from the inner accretion disk of a neutron star LMXB Serpens X-1 (ref. 86). The *x*-axis shows the X-ray energy and the *y*-axis gives the observed intensity in excess to the best-fit continuum spectral model. The data-points (shown with error bars) clearly show an asymmetric spectral line, while the dotted profile is a relativistic model of spectral line that fits the observed line well.

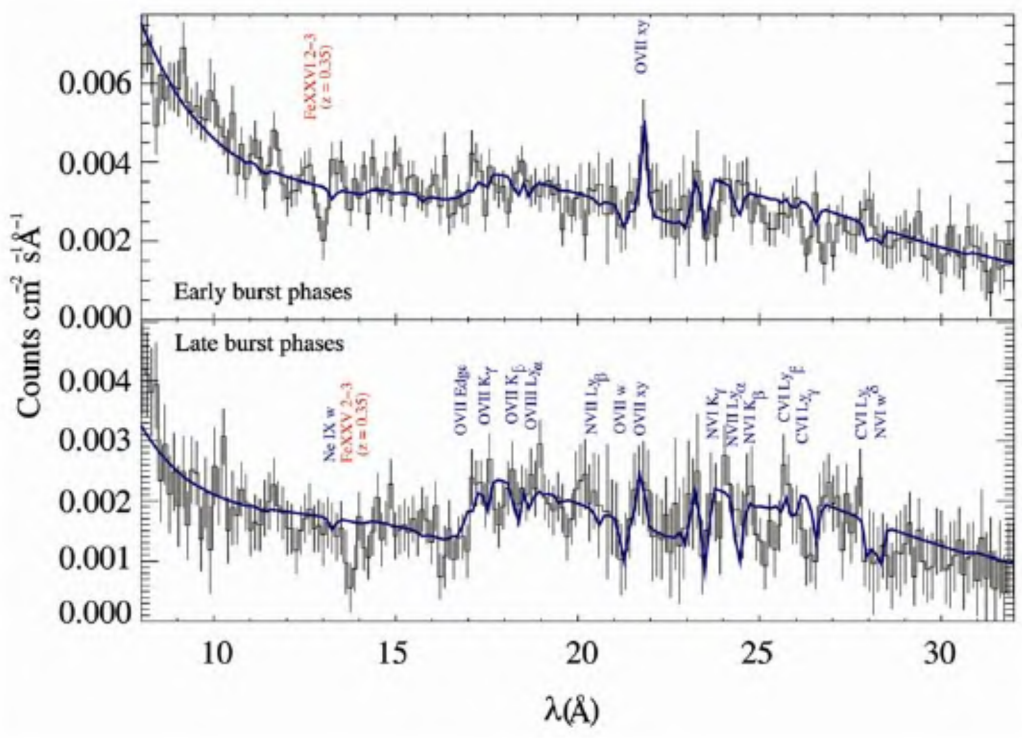

Figure 7. The total background-subtracted *XMM-Newton* RGS energy spectra (intensity vs wavelength) of the neutron star LMXB EXO 0748-676 during 28 thermonuclear X-ray bursts. The data are plotted as the black histograms with 1σ error bars. The blue line is the empirical continuum, with additional O VII intercombination line emission, modulated by absorption in photoionized circumstellar material. (Upper panel) Early burst phases (when the burst intensity is more). (Lower panel) Late burst phases (when the burst intensity is less). The two red labels indicate the iron absorption lines at a gravitational redshift $z = 0.35$, plausibly originated from the neutron star atmosphere (Figure courtesy: Mariano Méndez[92]).

photons (different from E_{em} because of the surface gravitational redshift), and M and R are the mass and the radius of the neutron star respectively. Note that the measurement of the stellar parameter R/M can be useful to understand the nature of the dense core matter of neutron stars. As the neutron stars in LMXB systems typically spin with high frequencies (~300–600 Hz), Doppler effect and special relativistic beaming should make the lines broad and asymmetric (similar to the lines from disks mentioned in the previous section). Measuring R/M accurately from such a broad line (for which the definition of E_{obs} is not certain) using the above formula is difficult. Bhattacharyya *et al.*[91] have recently suggested a way to measure the stellar R/M using the above formula from such lines. These broad asymmetric lines can have low-energy and high-energy peaks (or dips for absorption lines). Bhattacharyya *et al.*[91] have found that the ratio of energy contents of these peaks (or, dips) contains information about the general relativistic frame-dragging. Therefore, surface atomic lines can be used to test the theory of general relativity in the strong gravity regime.

Surface lines are likely to be detected from thermonuclear X-ray bursts and hence from neutron stars in LMXB systems. This is because: (1) the continuous accretion and the radiative pressure may keep the line-forming heavy elements in the stellar atmosphere for the time duration required for the line detection; (2) the relatively low magnetic fields (~10^7–10^9 Gauss) of the neutron stars in LMXBs should make the line of identification easier by keeping the magnetic splitting negligible; (3) the lower magnetic field does not complicate the modelling of the atmosphere; (4) the luminous bursts give good signal-to-noise ratio, and (5) during the bursts, typically 90% of the total emission originates from the neutron star surface, and hence the surface spectral line may be largely free from the uncertainty due to the other X-ray emission components, such as the accretion disk.

Indeed, the only plausible observation of the neutron star surface atomic spectral lines was from an LMXB EXO 0748-676 (ref. 92). These authors detected two significant absorption features in the *XMM-Newton* RGS energy spectra of the thermonuclear X-ray bursts, which they identified as Fe XXVI and Fe XXV $n = 2$–3 lines with a redshift of $z = 0.35$ (see Figure 7). In order to detect these lines, they had to combine the spectra of 28 bursts. The identification of these two lines as the surface atomic spectral lines is reasonable for the following reasons: (1) the early burst phases (when the temperature was higher) showed the Fe XXVI line, while the late burst phases (when the temperature was lower) showed

the Fe XXV line. This is consistent with qualitative temperature dependence of the iron ionization states. (2) The narrow lines were consistent with the relatively slow spin rate of the neutron star (45 Hz)[93]. (3) Both the lines showed the same surface gravitational redshift as expected. This redshift is reasonable for the surface of a typical neutron star. The absorption of some of the bursts photons (originated in deep burning layers) by the iron ions in the upper atmosphere might give rise to these redshifted lines. Chang *et al.*[94] showed that the observed strength of the iron lines could be produced by a neutron star photospheric metallicity, which was 2–3 times larger than the solar metallicity. However, these lines were not significantly detected from the new data from the later observations of the same source. Although this casts doubts about the reality of these lines, it may be caused by the change in the photospheric conditions that might weaken the lines. Therefore, the evidence of the existence of surface atomic lines currently remains uncertain, which, given the importance of these lines, provides the motivation for the future generation X-ray instruments.

Timing aspects

Colour–colour diagram

A convenient way to study how the persistent spectrum of a neutron star LMXB changes with time, and how it is correlated with various timing properties and the occurrence of other features (e.g. thermonuclear X-ray bursts), is to compute the colour–colour diagram. In order to do this, typically five photon energies with increasing values are considered: $h\nu_1$, $h\nu_2$, $h\nu_3$, $h\nu_4$ and $h\nu_5$. Let us assume that the observed background-subtracted photon count numbers in the ranges $h\nu_1 - h\nu_2$, $h\nu_2 - h\nu_3$, $h\nu_3 - h\nu_4$ and $h\nu_4 - h\nu_5$ are N_1, N_2, N_3 and N_4 respectively. Then we define soft colour = N_2/N_1 and hard colour = N_4/N_3. The colour–colour diagram is a plot of hard colour vs soft colour, which shows the change of spectral hardness of the source. Neutron star LMXBs can be divided into two classes based on their colour–colour diagrams: the so called 'Z sources' that show distinct Z-like curves (Figure 8), and the 'atoll sources' that exhibit C-like curves (Figure 9). These two types of curves are not only different by shape, but also they are correlated with distinctly different timing properties[95]. Apart from these differences, the Z sources are luminous (luminosities are close to Eddington), while the luminosities of the atoll sources typically remain between 0.01 and 0.2 of the Eddington luminosity[95]. The three branches of a Z curve, from upper to lower, are called horizontal branch (HB), normal branch (NB) and flaring branch (FB). The lower part of a typical atoll curve is called the banana state, while the upper part is known as the island state. The X-ray luminosity typically increases from HB to FB for a Z source, and from island state to banana state for an atoll source. We note that although the various characteristics of the colour–colour diagrams are observationally robust, most of them are not yet theoretically well understood. Accretion rate is known to be a parameter that changes along the Z curves and the atoll curves. But, given the complex properties of these curves, more parameters must be involved in the fundamental level. It is also not understood what apart from the accretion rate distinguishes between the Z and atoll properties. The recent discovery of the

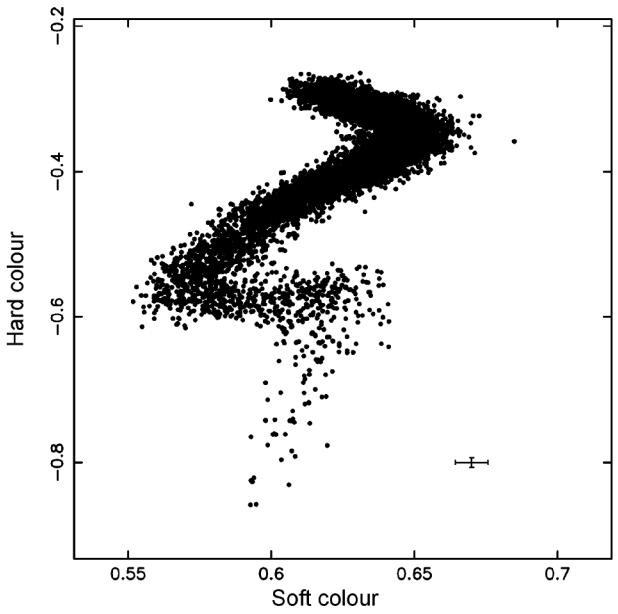

Figure 8. Typical colour–colour diagram (see text for the definition) of the members of the 'Z' subdivision of neutron star LMXBs. Such a diagram shows the evolution of the source spectral state (Figure courtesy: Peter Jonker[113]).

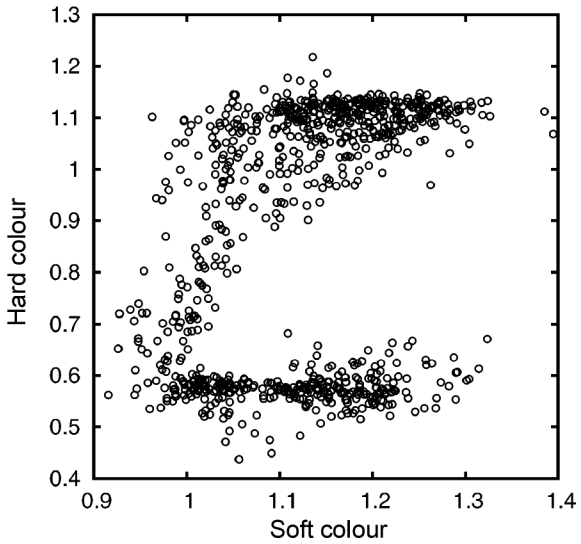

Figure 9. Typical colour–colour diagram (see text for the definition) of the members of the 'atoll' subdivision of neutron star LMXBs (figure courtesy: Diego Altamirano; van Straaten *et al.*[114]; Altamirano *et al.*[115]).

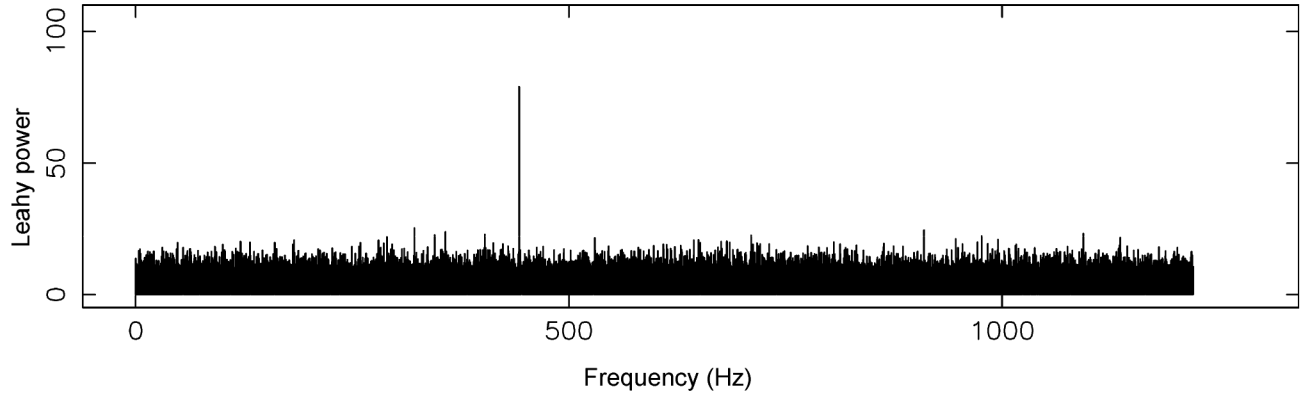

Figure 10. Power spectrum (i.e. Fourier transform of the observed X-ray intensity profile) of a neutron star LMXB. The peak at 442.36 Hz implies that (1) there is a periodic intensity variation with that frequency; (2) this source is an accretion-powered millisecond pulsar (see text); and (3) the spin frequency of the neutron star is 442.36 Hz (Figure courtesy: Diego Altamirano; Altamirano *et al.*[116]).

first transient Z source, that shows substantially changed properties at lower luminosities, holds the promise to take our understanding of these sources to a higher level[96].

Regular pulsations

Most of the radio pulsars (that are spinning neutron stars emitting periodic radio pulses) have spin period >10 ms, and high magnetic field (typically ~10^{12}–10^{13} Gauss). These are relatively young neutron stars. This is because, as a pulsar spins down (due to magnetic dipole radiation) and its magnetic field decays (in timescales of several million years), it eventually ceases to be a pulsar[97]. However, a small fraction of the radio pulsar population is rapidly spinning (period < 10 ms), old (age ~ billions of years), and having weak surface magnetic fields (10^8–10^9 Gauss). Since many of these pulsars are in binary systems, it has been believed for long time that these neutron stars were spun up by the accretion-induced angular momentum transfer in LMXB systems[97]. This model would be supported by the observation of millisecond-period X-ray pulsations from neutron star LMXBs, as such pulsations would be a missing link between the millisecond radio pulsars and LMXBs. But years of searching did not yield the detection of any such coherent millisecondperiod X-ray pulsations. Finally in 1998, the first millisecond X-ray pulsations (with the frequency ≈401 Hz) were discovered from the transient LMXB SAX J1808.4-3658 with the *RXTE* satellite[98]. As X-ray pulsations (like the radio pulsations) measure the neutron star spin frequency, this showed that the neutron star in this source spins with ≈401 Hz, and hence, indeed the neutron stars in the LMXBs can be spun up. Several such sources have been discovered after SAX J1808.4-3658 (see, for example, Wijnands[99], and Watts *et al.*[100]). Figure 10 shows the power spectrum of one such LMXB. The narrow peak at the frequency of 442.36 Hz shows the pulsations. Note that the computation of a power spectrum is a convenient way to detect timing features. Such a spectrum (power vs frequency) is a Fourier transform of the intensity profile (photon counts vs time). For example, if x_j ($j = 0, \ldots, N-1$) is the number of photons detected in bin j, then the discrete Fourier transform p_k ($k = -N/2, \ldots, N/2-1$) decomposes the intensity into N sine waves. The direct and the inverse Fourier transforms are then given by:

$$p_k = \sum_{j=0}^{N-1} x_j e^{2\pi i k j/N}; \; x_j = \frac{1}{N} \sum_{k=-N/2}^{N/2-1} p_k e^{-2\pi i k j/N}. \qquad (17)$$

In the LMXBs containing these pulsars, the accretion flow is channelled by the neutron star magnetic field to the magnetic polar cap. The X-ray hotspot on the neutron star created by this channelled flow rotates around the stellar spin axis (if the magnetic axis and the spin axis are misaligned) and gives rise to the observed X-ray pulses. Since the gravitational energy release from the accreted matter powers the X-ray pulsations, these sources are called 'accretion-powered millisecond pulsars' (AMPs). Since the first discovery of these pulsars, it intrigues the astrophysicists how these sources are different from other LMXBs, and why all the LMXBs do not exhibit such regular pulsations. The recent discovery of several intermittent AMPs (that show sporadic regular pulsations) holds the promise to resolve these problems[100]. Better understanding of the AMPs will be important to probe the evolution of LMXBs, as well as to model the magnetically channelled flows in the strong gravity regions near the neutron stars. Modelling of this flow, its energy spectrum and the timing properties will be useful to constrain the neutron star parameters, and hence the nature of the stellar core matter[101].

Burst oscillations

High frequency timing features are observed from many (so far about 20) neutron star LMXBs during thermonu-

clear X-ray bursts[27]. They are called 'burst oscillations', and were first discovered with the *RXTE* PCA instrument in bursts from the LMXB 4U 1728-34 (ref. 102). It was soon realized that this timing feature might be originated from an asymmetric brightness pattern on the surface of a spinning neutron star. This was confirmed when burst oscillations were detected from the AMP SAX J1808.4-3658 close to the known neutron star spin frequency[103]. Later, these oscillations were observed from other AMPs near the known stellar spin rates[100,104]. These established a new technique to measure the neutron star spin frequency. In fact, regular pulsations and burst oscillations are the only methods to measure the spin rates of neutron stars in LMXBs, and together they have provided spin frequencies of about 25 sources. Apart from measuring the stellar spin, the modelling of shapes and amplitudes of the phase-folded burst oscillation intensity profiles can be useful to constrain the other neutron star parameters (including the radius-to-mass ratio; e.g. Bhattacharyya *et al.*[105]). Figure 11 shows the burst oscillation power contours and the power spectrum for a neutron star LMXB. The power contours indicate that the oscillation frequency changes with time. Indeed such small evolution of frequencies is observed for many bursts, which suggests that the asymmetric brightness pattern slowly moves on the spinning neutron star surfaces. It is not yet understood what causes such motion, although several models exist in the literature[27]. The oscillations during burst rise are normally believed to be caused by the expansion of the burning region on the stellar surface immediately after the ignition. Therefore, the study of the evolution of the burst oscillation properties during burst rise can be useful to probe the thermonuclear flame-spreading. The nature of the asymmetric brightness pattern that causes the oscillations during burst decay is not yet well understood. This is because the entire stellar surface is believed to be ignited at this time. The existing models involve non-radial global oscillations in the surface layers[106], shear oscillations[107], etc. each of which has shortcomings.

Quasi-periodic oscillations and broadband power spectrum

Neutron star LMXBs show a variety of observationally robust timing features, many of which are not well understood yet. Continuum power, in excess of the mean random power, is often observed at frequencies less than 100 Hz. The nature of this power depends on the source state determined from the position on the colour–colour plot. For example, a power law-like continuum ($\propto \nu^{-\alpha}$; ν is the frequency in the power spectrum, and α a constant) below 1 Hz is typically dominant for the atoll sources in the end part of the banana state[95]. Apart from the broad continua, neutron star LMXBs often exhibit peaked features with a wide range of frequencies (millihertz to kilohertz). Since they are somewhat broad, and hence not quite periodic, these features are known as quasi-periodic oscillations (QPOs). Similar to the continuum features, QPOs are correlated with the colour–colour diagram. For example, a type of 15–60 Hz QPO appears in the horizontal branch of the colour–colour diagram of Z sources, and hence known as the 'horizontal branch oscillation' (HBO). The QPOs, when modelled correctly, are expected to significantly enhance our understanding of neutron star LMXBs. The observed correlations among different types of QPOs can be helpful for their modelling. However, in this short review we will not discuss the QPOs and their correlations in detail, and we refer to an extensive review by van der Klis[95] that gives a large amount of information about the fast X-ray timing properties of neutron star LMXBs. The only QPOs that we would like to briefly discuss here are called kilohertz (kHz) QPOs. These high-frequency QPOs are observed from both Z and atoll sources. The frequencies of kHz

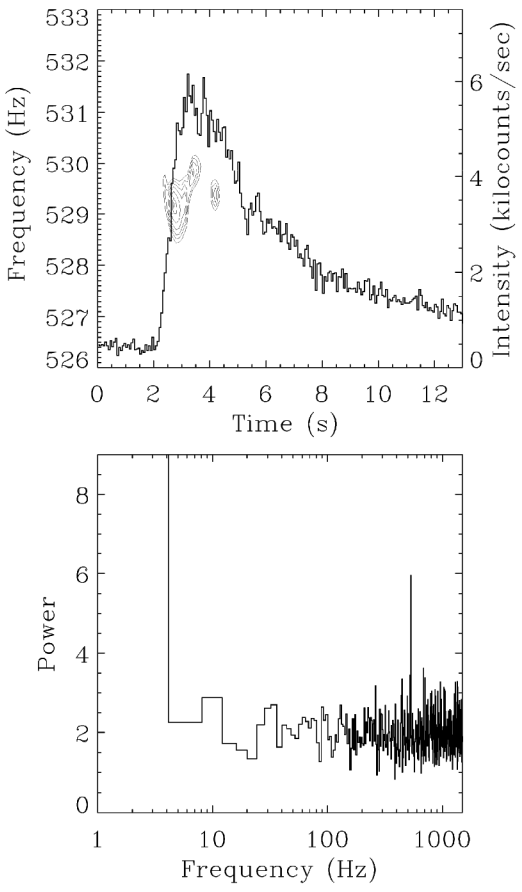

Figure 11. Upper panel: X-ray intensity profile of a thermonuclear X-ray burst from the neutron star LMXB 1A 1744-361 (ref. 112). Power contours around 530 Hz (calculated by Fourier transform) imply that there is a significant intensity variation (burst oscillation) with ≈530 Hz frequency. Note that the shape of the power contours indicates a slight change in frequency with time, which is common for burst oscillation. (Lower panel) The corresponding power spectrum. The peak at ≈530 Hz implies the burst oscillation with that frequency.

QPOs vary between ≈200 and 1200 Hz, and often they appear in a pair (see Figure 12). For a given source, the lower and upper kHz QPOs are seen to move up and down in frequency together, without changing the frequency separation much. This frequency separation is normally found to be within 20% of the neutron star spin frequency, or half of that, depending on the source. These kHz QPOs are believed to have originated from a region close to the neutron star, and hence, when their origin is fully understood, will be useful to measure the neutron star parameters, and to test the theory of general relativity (e.g., refs 108–110).

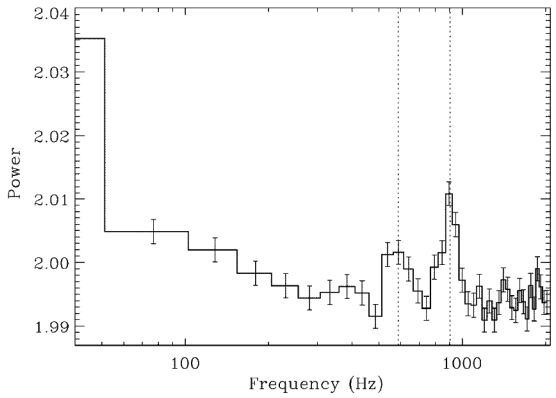

Figure 12. Power spectrum (i.e. Fourier transform of the observed X-ray intensity profile) of a neutron star LMXB showing a pair of kHz QPOs (see text). The vertical dotted lines show the centroid frequencies of these QPOs.

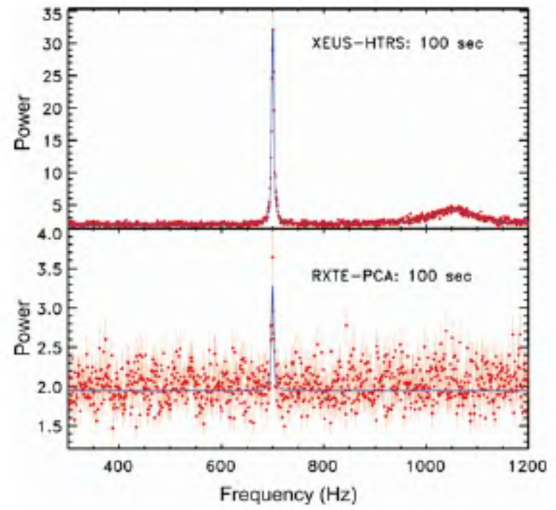

Figure 13. A comparison of a power spectrum observed with two (one current and one future) instruments. (Lower panel) Lower kHz QPO is barely detected and the upper kHz QPO is not detected from the power spectrum created from an intensity profile of 100 s duration observed with the PCA instrument of the *RXTE* satellite. (Upper panel) If the same observation were made with the High Time Resolution Spectrometer (previously proposed for the *X-Ray Evolving Universe Spectrometer* (*XEUS*), but now proposed for the *International X-ray Observatory* (*IXO*)), both the kHz QPOs would be significantly detected (Figure courtesy: Didier Barret; Barret[117]).

Future prospects

Neutron star LMXBs provide a unique opportunity to study several aspects of extreme physics that we have briefly discussed in this short review. These include: (1) constraining the equation-of-state models of the supranuclear density matter of neutron star cores from the measurements of the stellar parameters; (2) testing the theory of general relativity; (3) understanding the physics of neutron star atmospheres, and (4) probing the accretion flow in the strong gravity region near the neutron stars. In addition, the X-ray study of neutron star LMXBs allows us (1) to understand the evolution of these binary systems; (2) probe the long-term accretion process and the structures of the accreted matter, and (3) find out how and why these systems are different from black hole LMXBs. Since the observed X-ray properties mentioned in this review can be used as tools to achieve these scientific goals, we need to understand these properties better, and explore (1) the correlations among them, and (2) their correlations with the observations in other wavelengths. These can be achieved with more sensitive X-ray instruments (typically with larger photon-collecting areas), and simultaneous observations in multiple wavelengths. It will also be required to monitor the entire sky frequently with high sensitivity in order to catch the transient neutron star LMXBs during their outbursts. Here we give a short description of some of the proposed future space missions with these capabilities.

The proposed Indian multiwavelength astronomy space mission *Astrosat* will observe simultaneously in a wide energy range (optical to hard X-ray of 100 keV). Apart from this unprecedented capability, its LAXPC instrument should be able to detect and measure the high frequency timing features, such as kHz QPOs and regular pulsations, for the first time in hard X-rays (say, up to ≈50 keV). Note that in its own time, LAXPC will probably be the only instrument capable of detecting the high-frequency features in the X-ray band.

The proposed next generation joint American, European and Japanese satellite *International X-ray Observatory* (*IXO*) will have several highly sensitive instruments that will take the X-ray study of neutron star LMXBs to a higher level. In Figure 13, we demonstrate how significant an improvement the high timing resolution spectrometer (HTRS) instrument of *IXO* will make over the *RXTE* PCA for the high-frequency timing observations. Moreover, Ray *et al.*[111] mention that the proposed *Advanced X-ray Timing Array* (*AXTAR*) satellite will have better capabilities than *IXO* for these timing observations. Finally, the Japanese mission *Monitor of All-sky X-ray Image* (*MAXI*) will monitor the X-ray sky in the 0.5–30 keV range with high sensitivity. Therefore, the study of the neutron star LMXBs is likely to remain an active and promising field in order to explore some aspects of extreme physics.

1. Giacconi, R., Gursky, H., Paolini, F. R. and Rossi, B. B., Evidence for X-rays from sources outside the solar system. *Phys. Rev. Lett.*, 1962, **9**, 439–443.
2. Baade, W. and Zwicky, F., Supernovae and cosmic rays. *Phys. Rev.*, 1934, **45**, 138.
3. Oppenheimer, J. R. and Volkoff, G. M., On massive neutron cores. *Phys. Rev.*, 1939, **55**, 374–381.
4. Hewish, A., Bell, S. J., Pilkington, J. D. H., Scott, P. F. and Collins, R. A., Observation of a rapidly pulsating radio source. *Nature*, 1968, **217**, 709–713.
5. Gold, T., Rotating neutron stars as the origin of the pulsating radio sources. *Nature*, 1968, **218**, 731–732.
6. Gold, T., Rotating neutron stars and the nature of pulsars. *Nature*, 1969, **221**, 25–27.
7. Shapiro, S. L. and Teukolsky, S. A., *Black Holes, White Dwarfs, and Neutron Stars: The Physics of Compact Objects*, A Wiley-Interscience Publication, New York, 1983.
8. Bagchi, M., Ray, S., Dey, M. and Dey, J., Evidence for strange stars from joint observation of harmonic absorption bands and of redshift. *MNRAS*, 2006, **368**, 971–975.
9. Lattimer, J. M. and Prakash, M., Neutron star observations: prognosis for equation of state constraints. *Phys. Rep.*, 2007, **442**, 109–165.
10. Mukhopadhyay, B., Growing hydrodynamic modes in Keplerian accretion disks during secondary Perturbations: elliptical vortex effects. *ApJ*, 2006, **653**, 503–512.
11. Mukhopadhyay, B., Afshordi, N. and Narayan, R., Bypass to turbulence in hydrodynamic accretion disks: an Eigenvalue approach. *ApJ*, 2005, **629**, 383–396.
12. Mukhopadhyay, B. and Misra, R., Pseudo-Newtonian potentials to describe the temporal effects on relativistic accretion disks around rotating black holes and neutron stars. *ApJ*, 2003, **582**, 347–351.
13. Ghosh, P., Pethick, C. J. and Lamb, F. K., Accretion by rotating magnetic neutron stars. I – Flow of matter inside the magnetosphere and its implications for spin-up and spin-down of the star. *ApJ*, 1977, **217**, 578–596.
14. Ghosh, P. and Lamb, F. K., Disk accretion by magnetic neutron stars. *ApJ*, 1978, **223**, L83–L87.
15. Ray, A. and Kembhavi, A., Thermal regeneration of neutron-star magnetic fields in binary radio and X-ray pulsars?. *MNRAS*, 1985, **217**, 753–760.
16. Srinivasan, G., Bhattacharya, D., Muslimov, A. G. and Tsygan, A. J., A novel mechanism for the decay of neutron star magnetic fields. *Curr. Sci.*, 1990, **59**, 31–38.
17. Jahan Miri, M. and Bhattacharya, D., Evolution of the magnetic fields of neutron stars in low-mass binary systems. *JApAS*, 1995, **16**, 231–233.
18. Konar, S., Bhattacharya, D. and Urpin, V., Evolution of the magnetic field of an accreting neutron star. *JApAS*, 1995, **16**, 249–250.
19. Choudhuri, A. R. and Konar, S., Diamagnetic screening of the magnetic field in accreting neutron stars. *MNRAS*, 2002, **332**, 933–944.
20. Konar, S. and Choudhuri, A. R., Diamagnetic screening of the magnetic field in accreting neutron stars – II. The effect of polar cap widening. *MNRAS*, 2004, **348**, 661–668.
21. Datta, B. and Kapoor, R. C., General relativistic effects on the pulse profile of fast pulsars. *Nature*, 1985, **315**, 557–559.
22. Liu, Q. Z., van Paradijs, J. and van den Heuvel, E. P. J., A catalogue of low-mass X-ray binaries in the Galaxy, LMC, and SMC (Fourth edition). *A&A*, 2007, **469**, 807–810.
23. Shakura, N. I. and Sunyaev, R. A., Black holes in binary systems. observational appearance. *A&A*, 1973, **24**, 337–355.
24. King, A. R., Kolb, U. and Burderi, L., Black hole binaries and X-ray transients. *ApJ*, 1996, **464**, L127–L130.
25. King, A. R., Disc instabilities in soft X-ray transients. Proceedings of the Jan van Paradijs Memorial Symposium, 2001.
26. Cackett, E. M., Wijnands, R., Miller, J. M., Brown, E. F. and Degenaar, N., Cooling of the crust in the Neutron star low-mass X-ray binary MXB 1659-29. *ApJ*, 2008, 687, L87–L90.
27. Strohmayer, T. E. and Bildsten, L., New views of thermonuclear bursts. In *Compact Stellar X-ray Sources* (eds Lewin, W. H. G. and van der Klis, M.), Cambridge University Press, Cambridge, 2006, pp. 113–156.
28. Grindlay, J. E. *et al.*, Discovery of intense X-ray bursts from the globular cluster NGC 6624. *ApJ*, 1976, **205**, L127–L130.
29. Belian, R. D., Conner, J. P. and Evans, W. D., The discovery of X-ray bursts from a region in the constellation Norma. *ApJ*, 1976, **206**, L135–L138.
30. Joss, P. C., X-ray bursts and neutron-star thermonuclear flashes. *Nature*, 1977, **270**, 310–314.
31. Lamb, D. Q. and Lamb, F. K., Nuclear burning in accreting neutron stars and X-ray bursts. *ApJ*, 1978, **220**, 291–302.
32. Swank, J. H., Becker, R. H., Boldt, E. A., Holt, S. S., Pravdo, S. H. and Serlemitsos, P. J., Spectral evolution of a long X-ray burst. *ApJ*, 1977, **212**, L73–L76.
33. Bildsten, L., Theory and observations of type I X-ray bursts from neutron stars. *AIP Conference Proceedings*, 2000, **522**, 359–369.
34. Hansen, C. J. and van Horn, H. M., Steady-state nuclear fusion in accreting neutron-star envelopes. *ApJ*, 1975, **195**, 735–741.
35. Fowler, W. A. and Hoyle, F., *Nucleosynthesis in massive stars and supernovae*, University of Chicago Press, Chicago, 1965.
36. Hanawa, T., Sugimoto, D. and Hashimoto, M., Nucleosynthesis in explosive hydrogen burning and its implications in ten-minute interval of X-ray bursts. *PASJ*, 1983, **35**, 491–506.
37. Hanawa, T. and Fujimoto, M. Y., Thermal response of neutron stars to shell flashes. *PASJ*, 1984, **36**, 199–214.
38. Koike, O., Hashimoto, M., Arai, K., Wanajo, S., Rapid proton capture on accreting neutron stars – effects of uncertainty in the nuclear process. *A&A*, 1999, **342**, 464–473.
39. Schatz, H., Bildsten, L., Cumming, A. and Wiescher, M., The rapid proton process ashes from stable nuclear burning on an accreting neutron star. *ApJ*, 1999, **524**, 1014–1029.
40. Schatz, H. *et al.*, End point of the rp process on accreting neutron stars. *PRL*, 2001, **86**, 3471–3474.
41. Wallace, R. K. and Woosley, S. E., Explosive hydrogen burning, *ApJS*, 1981, **43**, 389–420.
42. Ayasli, S. and Joss, P. C., Thermonuclear processes on accreting neutron stars – A systematic study. *ApJ*, 1982, **256**, 637–665.
43. Taam, R. E., Woosley, S. E. and Lamb, D. Q., The Effect of Deep Hydrogen burning in the accreted envelope of a neutron star on the properties of X-ray bursts. *ApJ*, 1996, **459**, 271–277.
44. Cornelisse, R., Heise, J., Kuulkers, E., Verbunt, F. and in't Zand, J. J. M., The longest thermonuclear X-ray burst ever observed?. A BeppoSAX Wide Field Camera observation of 4U 1735-44. *A&A*, 2000, **357**, L21–L24.
45. Cooper, R. L., Steiner, A. W. and Brown, E. F., Possible Resonances in the 12C + 12C fusion rate and superburst ignition. *ApJ*, 2009, **702**, 660–671.
46. Cumming, A. and Bildsten, L., Carbon flashes in the heavy-element ocean on accreting neutron stars. *ApJ*, 2001, **559**, L127–L130.
47. Strohmayer, T. E. and Brown, E. F., A remarkable 3 hour thermonuclear burst from 4U 1820–30. *ApJ*, 2002, **566**, 1045–1059.
48. Fryxell, B. A. and Woosley, S. E., A two-dimensional model for gamma-ray bursts. *ApJ*, 1982, **258**, 733–739.
49. Spitkovsky, A., Levin, Y. and Ushomirsky, G., Propagation of thermonuclear flames on rapidly rotating neutron stars: extreme weather during type I X-ray bursts. *ApJ*, 2002, **566**, 1018–1038.
50. Bhattacharyya, S. and Strohmayer, T. E., A non-PRE double-peaked burst from 4U 1636–536: evidence of burning front propagation. *ApJ*, 2006, **636**, L121–L124.

51. Bhattacharyya, S. and Strohmayer, T. E., Spreading of thermonuclear flames on the neutron star in SAX J1808.4-3658: an observational tool. *ApJ*, 2006, **642**, L161–L164.
52. Bhattacharyya, S. and Strohmayer, T. E., An unusual precursor burst with oscillations from SAX J1808.4-3658. *ApJ*, 2007, **656**, 414–419.
53. Bhattacharyya, S. and Strohmayer, T. E., Thermonuclear flame spreading on rapidly spinning neutron stars: indications of the coriolis force?. *ApJ*, 2007, **666**, L85–L88.
54. Lewin, W. H. G. *et al.*, The discovery of rapidly repetitive X-ray bursts from a new source in Scorpius. *ApJ*, 1976, **207**, L95–L99.
55. Lewin, W. H. G., Rutledge, R. E., Kommers, J. M., van Paradijs, J. and Kouveliotou, C., A comparison between the rapid burster and GRO J1744-28. *ApJ*, 1996, **462**, L39–L42.
56. Fishman, G. J. *et al.*, Galactic Center, IAU Circ., 1995, 6272, 1.
57. Lewin, W. H. G., van Paradijs, J. and Taam, R. E., X-ray bursts. In *X-ray Bimaries* (eds Lewin, W. H. G., van Paradijs, J. and van den Heuvel, E. P. J.), Cambridge University Press, Cambridge, 1995, pp. 175–232.
58. Spruit, H. C. and Taam, R. E., An instability associated with a magnetosphere–disk interaction. *ApJ*, 1993, **402**, 593–604.
59. Mahasena, P. *et al.*, New results from ASCA on the type II bursts of the rapid burster (MXB 1730-335). *PASJ*, 2003, **55**, 827–840.
60. White, N. E. and Mason, K. O., The structure of low-mass X-ray binaries. *Space Sci. Rev.*, 1985, **40**, 167–194.
61. Parmar, A. N., White, N. E., Giommi, P. and Gottwald, M., The discovery of 3.8 hour periodic intensity dips and eclipses from the transient low-mass X-ray binary EXO 0748-676. *ApJ*, 1986, **308**, 199–212.
62. Frank, J., King, A. R. and Lasota, J.-P., The light curves of low-mass X-ray binaries. *A&A*, 1987, **178**, 137–142.
63. White, N. E. and Swank, J. H., The discovery of 50 minute periodic absorption events from 4U 1915–05. *ApJ*, 1982, **253**, L61–L66.
64. Mitsuda, K. *et al.*, Energy spectra of low-mass binary X-ray sources observed from TENMA. *PASJ*, 1984, **36**, 741–759.
65. White, N. E., Peacock, A. and Taylor, B. G., EXOSAT observations of broad iron K line emission from Scorpius X-1. *ApJ*, 1985, **296**, 475–480.
66. White, N. E. *et al.*, A study of the continuum and iron K line emission from low-mass X-ray binaries. *MNRAS*, 1986, **218**, 129–138.
67. Bhattacharyya, S., Strohmayer, T. E., Swank, J. H. and Markwardt, C. B., RXTE observations of 1A 1744-361: correlated spectral and timing behavior. *ApJ*, 2006, **652**, 603–609.
68. Church, M. J. *et al.*, Simple photoelectric absorption during dipping in the ASCA observation of XB 1916-053. *ApJ*, 1997, **491**, 388–394.
69. Galloway, D. K., Muno, M. P., Hartman, J. M., Psaltis, D., Chakrabarty, D., Thermonuclear (Type I) X-ray bursts observed by the Rossi X-ray timing explorer. *ApJS*, 2008, **179**, 360–422.
70. Hoffman, J. A., Lewin, W. H. G. and Doty, J., Observations of the X-ray burst source MXB 1636-53. *ApJ*, 1977, **217**, L23–L28.
71. London, R. A., Howard, W. M. and Taam, R. E., The spectra of X-ray bursting neutron stars. *ApJ*, 1984, **287**, L27–L30.
72. London, R. A., Howard, W. M. and Taam, R. E., Model atmospheres for X-ray bursting neutron stars. *ApJ*, 1986, **306**, 170–182.
73. Ebisuzaki, T. and Nakamura, N., The difference in hydrogen abundance between two classes of type I X-ray bursts. *ApJ*, 1988, **328**, 251–255.
74. Madej, J., Model atmospheres and X-ray spectra of bursting neutron stars. *ApJ*, 1991, **376**, 161–176.
75. Titarchuk, L., On the spectra of X-ray bursters: expansion and contraction stages. *ApJ*, 1994, **429**, 340–355.
76. Madej, J., Joss, P. C. and Różańska, A., Model atmospheres and X-ray spectra of bursting neutron stars: hydrogen–helium comptonized spectra. *ApJ*, 2004, **602**, 904–912.
77. Boirin, L., Méndez, M., Díaz Trigo, M., Parmar, A. N. and Kaastra, J. S., A highly-ionized absorber in the X-ray binary 4U 1323-62: a new explanation for the dipping phenomenon. *A&A*, 2005, **436**, 195–208.
78. Boirin, L., Parmar, A. N., Barret, D., Paltani, S. and Grindlay, J. E., Discovery of X-ray absorption features from the dipping low-mass X-ray binary XB 1916-053 with XMM-Newton. *A&A*, 2004, **418**, 1061–1072.
79. Parmar, A. N., Oosterbroek, T., Boirin, L. and Lumb, D., Discovery of narrow X-ray absorption features from the dipping low-mass X-ray binary X 1624-490 with XMM-Newton. *A&A*, 2002, **386**, 910–915.
80. Díaz Trigo, M., Parmar, A. N., Boirin, L., Méndez, M. and Kaastra, J. S., Spectral changes during dipping in low-mass X-ray binaries due to highly-ionized absorbers. *A&A*, 2006, **445**, 179–195.
81. Jimenez-Garate, M. A., Schulz, N. S. and Marshall, H. L., Discrete X-ray signatures of a photoionized plasma above the accretion disk of the neutron star EXO 0748-676. *ApJ*, 2003, **590**, 432–444.
82. Reynolds, C. S. and Nowak, M. A., Fluorescent iron lines as a probe of astrophysical black hole systems. *Phys. Rep.*, 2003, **377**, 389–466.
83. Miller, J. M., A short review of relativistic iron lines from stellar-mass black holes. *Astronomische Nachrichten*, 2006, **327**, 997–1003.
84. Fabian, A. C., Iwasawa, K., Reynolds, C. S. and Young, A. J., Broad iron lines in active galactic nuclei. *PASP*, 2000, **112**, 1145–1161.
85. Asai, K., Dotani, T., Nagase, F. and Mitsuda, K., Iron K emission lines in the energy spectra of low-mass X-ray binaries observed with ASCA. *ApJSS*, 2000, **131**, 571–591.
86. Bhattacharyya, S. and Strohmayer, T. E., Evidence of a broad relativistic iron line from the neutron star low-mass X-ray binary serpens X-1. *ApJ*, 2007, **664**, L103–L106.
87. Cackett, E. M. *et al.*, Relativistic iron emission lines in neutron star low-mass X-ray binaries as probes of neutron star radii. *ApJ*, 2008, **674**, 415–420.
88. Pandel, D., Kaaret, P. and Corbel, S., Relativistic iron line emission from the neutron star low-mass X-ray binary 4U 1636-536. *ApJ*, 2008, **688**, 1288–1294.
89. Di Salvo, T. *et al.*, A relativistically smeared spectrum in the neutron star X-ray binary 4U 1705-44: looking at the inner accretion disc with X-ray spectroscopy. *MNRAS*, 2009, in press.
90. Özel, F. and Psaltis, D., Spectral lines from rotating neutron stars. *ApJ*, 2003, **582**, L31–L34.
91. Bhattacharyya, S., Miller, M. C. and Lamb, F. K., The Shapes of atomic lines from the surfaces of weakly magnetic rotating neutron stars and their implications. *ApJ*, 2006, **644**, 1085–1089.
92. Cottam, J., Paerels, F. and Méndez, M., Gravitationally redshifted absorption lines in the X-ray burst spectra of a neutron star. *Nature*, 2002, **420**, 51–54.
93. Villarreal, A. R. and Strohmayer, T. E., Discovery of the neutron star spin frequency in EXO 0748-676. *ApJ*, 2004, **614**, L121–L124.
94. Chang, P., Bildsten, L. and Wasserman, I., Formation of resonant atomic lines during thermonuclear flashes on neutron stars. *ApJ*, 2005, **629**, 998–1007.
95. van der Klis, M., Rapid X-ray variability. In *Compact Stellar X-ray Sources* (eds Lewin, W. H. G. and van der Klis, M.), Cambridge University Press, Cambridge, 2006, pp. 39–112.
96. Homan, J. *et al.*, Rossi X-ray timing explorer observations of the first transient Z source XTE J1701-462: shedding new light on mass accretion in luminous neutron star X-ray binaries. *ApJ*, 2007, **656**, 420–430.

97. Bhattacharya, D. and van den Heuvel, E. P. J., Formation and evolution of binary and millisecond radio pulsars. *Phys. Rep.*, 1991, **203**, 1–124.
98. Wijnands, R. and van der Klis, M., A millisecond pulsar in an X-ray binary system. *Nature*, 1998, **394**, 344–346.
99. Wijnands, R., Accretion-driven millisecond X-ray pulsars. In *Trends in Pulsar Research* (ed. Lowry, J. A.), Nova Science Publishers, Inc, New York, 2006, p. 53.
100. Watts, A. L. *et al.*, Discovery of burst oscillations in the intermittent accretion-powered millisecond pulsar HETE J1900.1-2455. *ApJ*, 2009, **698**, L174–L177.
101. Poutanen, J. and Gierliński, M., On the nature of the X-ray emission from the accreting millisecond pulsar SAX J1808.4-3658. *MNRAS*, 2003, **343**, 1301–1311.
102. Strohmayer, T. E. *et al.*, Millisecond X-ray variability from an accreting neutron star system. *ApJ*, 1996, **469**, L9–L12.
103. Chakrabarty, D. *et al.*, Nuclear-powered millisecond pulsars and the maximum spin frequency of neutron stars. *Nature*, 2003, **424**, 42–44.
104. Strohmayer, T. E., Markwardt, C. B., Swank, J. H. and in't Zand, J., X-ray bursts from the accreting millisecond pulsar XTE J1814-338. *ApJ*, 2003, **596**, L67–L70.
105. Bhattacharyya, S., Strohmayer, T. E., Miller, M. C. and Markwardt, C. B., Constraints on neutron star parameters from burst oscillation light curves of the accreting millisecond pulsar XTE J1814-338. *ApJ*, 2005, **619**, 483–491.
106. Heyl, J., r-Modes on rapidly rotating, relativistic stars. I. Do type I bursts excite modes in the neutron star ocean?. *ApJ*, 2004, **600**, 939–945.
107. Cumming, A., Latitudinal shear instabilities during type I X-ray bursts. *ApJ*, 2005, **630**, 441–453.
108. Miller, M. C., Lamb, F. K. and Psaltis, D., Sonic-point model of kilohertz quasi-periodic brightness oscillations in low-mass X-ray binaries. *ApJ*, 1998, **508**, 791–830.
109. Stella, L. and Vietri, M., Lense-thirring precession and quasi-periodic oscillations in low-mass X-ray binaries. *ApJ*, 1998, **492**, L59–L62.
110. Barret, D., Olive, J.-F. and Miller, M. C., Drop of coherence of the lower kilo-Hz QPO in neutron stars: Is there a link with the innermost stable circular orbit? *Astronomische Nachrichten*, 2005, **326**, 808–811.
111. Ray, P. S., Chakrabarty, D., Strohmayer, T. E. and AXTAR Collaboration, The advanced X-ray timing array (AXTAR). *Bull. Am. Astron. Soc.*, 2009, **41**, 347–347.
112. Bhattacharyya, S., Strohmayer, T. E., Markwardt, C. B. and Swank, J. H., The discovery of a neutron star with a spin frequency of 530 Hz in A1744-361. *ApJ*, 2006, **639**, L31–L34.
113. Jonker, P. G., Wijnands, R., van der Klis, M., Psaltis, D., Kuulkers, E. and Lamb, F. K., Discovery of kilohertz quasi-periodic oscillations in the Z source GX 340 + 0. *ApJ*, 1998, **499**, L191–L194.
114. van Straaten, S., van der Klis, M. and Méndez, M., The atoll source states of 4U 1608-52. *ApJ*, 2003, **596**, 1155–1176.
115. Altamirano, D., van der Klis, M., Méndez, M., Wijnands, R., Markwardt, C. and Swank, J., Discovery of kilohertz quasi-periodic oscillations and state transitions in the low-mass X-ray binary 1E 1724-3045 (Terzan 2). *ApJ*, 2008, **687**, 488–504.
116. Altamirano, D., Casella, P., Patruno, A., Wijnands, R. and van der Klis, M., Intermittent millisecond X-ray pulsations from the neutron star X-ray transient SAX J1748.9-2021 in the globular cluster NGC 6440. *ApJ*, 2008, **674**, L45–L48.
117. Barret, D. *et al.*, Science with the XEUS high time resolution spectrometer. *SPIE*, 2008, **7011**, 1–10.